Nonexponential Kinetics of DNA Escape from α-Hemolysin Nanopores

Matthew Wiggin,*† Carolina Tropini,† Vincent Tabard-Cossa,† Nahid N. Jetha,† and Andre Marziali†
*Department of Biochemistry & Molecular Biology, and †Department of Physics & Astronomy, University of British Columbia, Vancouver, British Columbia, Canada

ABSTRACT Throughput and resolution of DNA sequence detection technologies employing nanometer scale pores hinge on accurate kinetic descriptions of DNA motion in nanopores. We present the first detailed experimental study of DNA escape kinetics from α-hemolysin nanopores and show that anomalously long escape times for some events result in nonexponential kinetics. From the distribution of first-passage times, we determine that the energy barrier to escape follows a Poisson-like distribution, most likely due to stochastic weak binding events between the DNA and amino acid residues in the pore.

INTRODUCTION

Nanometer-scale pores in insulating membranes, or nanopores, are increasingly being employed for detection of specific biomolecules, and for measurement of their physical properties. The reduction or fluctuation of ionic current when a charged molecule is driven into the pore by an electric field indicates the presence of the molecule and can provide either static or dynamic structural information (1–3).

Variations on this fundamental method are now used widely for analysis of nucleic acids, particularly for rapid sequence specific DNA detection (4,5). Though simple ionic current measurements are not viewed as promising for DNA sequencing (5,6), many other schemes have been explored, including reading DNA or RNA block copolymer sequences (7,8), sequencing by electronic measurements using sensors embedded in solid state nanopores (9,10), and genotyping by force spectroscopy either on dsDNA (11,12), or dsDNA-restriction enzyme complexes (13). All of these methods rely on moving DNA through the pore; their feasibility therefore hinges on a detailed understanding of the kinetics of DNA motion in nanopores.

Though considerable work on kinetics exists (8,14–20), unresolved questions remain. A fundamental issue concerns the distribution of first-passage times for DNA escaping from a state where it is threaded through a pore. Careful examination of published experimental translocation data frequently reveals a significant number of unexpectedly long escape events (17,21), leading to long tails in first-passage time distributions. We have observed similar long-tailed kinetics in our nanopore force spectroscopy work (11,12), which uses single molecule dissociation time-distributions to estimate sequence homology between single-stranded DNA (ssDNA) molecules, and in force spectroscopy data published by other groups (22,23).

Our current work explores escape kinetics in detail. We electrophoretically insert an ssDNA molecule coupled to Avidin into an α-hemolysin nanopore (α-HL) and subsequently allow it to escape thermally against an electrostatic potential (Fig. 1). This experiment is simplified from previous work on DNA duplex force spectroscopy (11,12), in that the electrostatic barrier and DNA-pore interactions are the only likely contributors to escape time. It is also simpler than translocation experiments: the time between polymer capture and entry of a free end into the pore (threading), shown to affect translocation time distributions (19), is decoupled from our measured escape time. We explore the relationship among kinetics, applied force, and ssDNA length, and find that although escape timescales obey Kramers' rule (24), the first-passage time distribution is nonexponential, indicating stochastic variation of the energy barrier height due to DNA-pore interactions.

MATERIALS AND METHODS

The α-HL pores are formed using a method adapted from that of Akeson et al. (7). Briefly, a black lipid membrane of 1,2-diphytanoyl-*sn*-glycero-3-phosphocholine (Avanti, Alabaster AL) and hexadecene (Sigma-Aldrich, St. Louis MO) is formed in a 25 μm PTFE aperture connecting two baths filled with 1 M KCl, 10 mM HEPES, pH 8.0 solution. Data collection is as described in previous work (11), with all data low-pass filtered at 10 kHz, and sampled at 50 kHz. Poly-dA DNA molecules, ranging in length from 15 to 65 bases were used (MWG Biotech, High Point, NC or IDT DNA, Coralville, IA). Unless otherwise stated, DNA was biotinylated and coupled to Avidin (Sigma Aldrich, Oakville, ON Canada) at the 3′ end. Molecules were verified by mass spectrometry, and not found to contain detectable quantities of truncated DNA.

We insert Avidin-labeled ssDNA into the *cis*-side of a single α-HL nanopore (CalBioChem, San Diego, CA) by applying a 200 mV capture potential across the pore. Avidin prevents full translocation of the DNA so that exit is always to the *cis*-side of the pore. A typical single molecule event is shown in Fig. 1.

For each sample, we observed escape times at ~10 different escape potentials recording between 100 and 10,000 single molecule events at every potential. Impedance is a very sensitive indicator of molecule conformation in α-HL nanopores (25,26). This provides some confidence that misthreaded molecules, or molecules with unusual conformations in the pore, would be easily detectable through significant changes in blocked current. We therefore discarded events whose current either deviated by >10 pA from the average at any time during the 100-ms capture phase, or did not immediately return to the open channel value upon molecule exit. The remaining events did not show

Submitted May 20, 2008, and accepted for publication August 5, 2008.

Address reprint requests to Dr. Andre Marziali, Tel.: 604-822-4514; E-mail: andre@phas.ubc.ca.

Editor: Taekjip Ha.

© 2008 by the Biophysical Society
0006-3495/08/12/5317/07 $2.00

doi: 10.1529/biophysj.108.137760

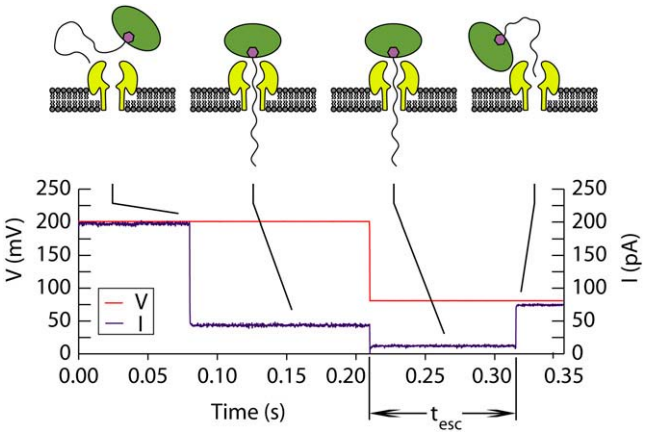

FIGURE 1 A single molecule escape event. Molecules are captured at 200 mV, resulting in increased impedance and decreased ionic current; the potential is then reduced to the escape potential (80 mV shown). The molecule undergoes thermally activated escape from the pore after a time t_{esc}. Rare events, lasting longer than 10 s, are terminated by reversing the potential and are not timed, but are counted in the total number of events for calculation of survival probability.

any correlation between event duration and impedance; we are confident that for these events the DNA molecule inserted properly into the pore.

For each dataset, we used the distribution of event durations to determine the survival probability as a function of time ($P_{survival}(t)$), i.e., the likelihood that a DNA molecule is still present in the pore at time t after the potential is reduced to the escape voltage.

RESULTS AND DISCUSSION

Fig. 2, *A* and *B*, show survival probability versus time for a 27-mer poly-dA molecule (dA27) at 80 mV (4783 escape events). At long times (≥0.1 s), it decays nonexponentially, following a power law. Nonexponential survival probability distributions were observed in all experiments, including molecules escaping in both orientations, i.e., 3′-first, and 5′-first (data not shown). We did not observe that the molecule's orientation had a significant effect on the escape time distribution. This is not surprising, given that escape kinetics are primarily determined by the electrostatic energy barrier, which is expected to be similar for molecules in both orientations.

We can exclude many possible causes for the nonexponential behavior based on results from control experiments, and from the relevant literature. It is unlikely that the nonexponential tail is caused by events where DNA is not properly threaded through the pore; as noted in Materials and Methods, even small changes in the position and length of a molecule in the pore have large effects on the pore conductance (25,26), and we discard events with noncharacteristic impedance from our data. Though DNA-lipid interactions and Avidin-pore interactions are also possible sources of energy barrier fluctuations, they cannot entirely account for our results, since molecules too short to protrude from the *trans*-side of the pore also exhibit nonexponential kinetics, as do molecules where Avidin is replaced by a DNA hairpin (data not shown).

Other groups have observed DNA hairpin escape from α-HL in the biased diffusion regime by applying negative potentials to assist the escape process. They reported exponential escape kinetics at large negative potentials (16), but nonexponential kinetics at small negative potentials (27). We note that these experiments, which explore electrically induced drift, are significantly different from our experiments, which explore escape over an electrostatic energy barrier.

The nonexponential decay of survival probability is surprising if one considers a one-dimensional diffusive model of the escape process. In such a model, the molecule escapes by diffusing along the axis of the pore against an electrostatic energy barrier. We model the escape process using the one-dimensional Fokker-Planck equation,

$$\frac{\partial}{\partial t} f(x,t) = D\frac{\partial^2}{\partial x^2} f(x,t) - \frac{\partial}{\partial x}\frac{F(x)}{\gamma} f(x,t), \qquad (1)$$

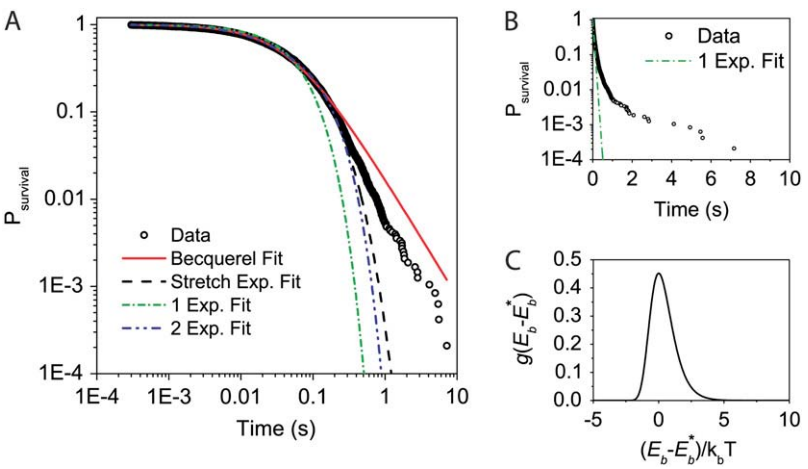

FIGURE 2 (*A*) Survival probability of dA27 trapped in the pore by an 80 mV applied potential (4783 events). The log-log plot emphasizes the long power law region between 0.1 and 10 s, and shows small variations between the data and fits at low $P_{survival}(t)$. Linearly weighted single exponential (one free parameter, $R^2 = 0.9763$), two-term exponential (three free parameters, $R^2 = 0.9993$), stretched exponential (two free parameters, $R^2 = 0.9993$), and Becquerel (two free parameters, $R^2 = 0.9982$) fits to the data are shown. While all fits presented, except the single exponential, describe the data with high R^2 values, only the Becquerel fit qualitatively reproduces the data at long times. The Becquerel fit yields the additional advantage of providing a simple analytic form for the distribution of energy barriers (Eq. 4) and timescales (Eq. 5). Characteristic timescales from all fits obey Kramers' law as the voltage is varied. (*B*) Semilog plot of the same data as in panel *A*, showing deviation from the exponential fit. (*C*) Calculated energy barrier height distribution for a 27-mer poly-dA molecule under an applied potential of 80 mV. $g(E_b\text{-}E_b^*)$ was calculated from Eq. 4, using parameters from a Becquerel fit to data in panel *A*. The FWHM of the distribution is ~2 k_BT. Note that energy is expressed relative to E_b^*, the energy at the peak of the distribution.

where $f(x,t)$ is the probability density function for the DNA molecule in the pore, with x indicating displacement from the starting location (with Avidin in contact with the *cis* mouth of the pore), and t indicating time. The value D is the one-dimensional diffusion coefficient, γ is a friction constant, and $F(x) = -dE(x)/dx$ is the force resulting from the applied electric potential, chain entropy, and other interactions which can all be included in a free energy profile $E(x)$ (assumed here to be time-invariant).

This model suggests that the survival probability $P_{\text{survival}}(t)$, which is the integral of $f(x,t)$ over the length of the DNA molecule, should decay exponentially at long times, regardless of the height of the energy barrier (see Appendix A). This can also be seen intuitively. For small barriers, Eq. 1 becomes the diffusion equation, with a solution composed of harmonic eigen-functions each of which decays exponentially in time. High frequency modes decay fastest, leading at long times to exponential probability decay governed by the lowest frequency mode. $P_{\text{survival}}(t)$ is therefore not expected to decay exponentially initially, but should convert to an exponential decay on a timescale dictated by the diffusion time over the length scale of the system (L^2/2D, where L is the length of the molecule). This initial relaxation time is <500 μs (18), which is fast compared to our experimental times. For large barriers, the system is quasistationary (28) and probability density leaks out over the barrier at a constant rate, leading to a single exponential decrease in the total remaining probability inside the pore. It is therefore surprising to see nonexponential probability decay at long times (>0.1 s) in our experiment, long after diffusive effects should have erased the memory of the initial probability distribution.

A barrier height that varies from event to event would lead to multiple timescales, making the probability distribution over many events nonexponential. We discuss possible causes for such a variation below. A coarse approximation of this, shown in Fig. 2 *A*, is a two-term exponential fit, which assumes that the molecule must escape over one of two distinct energy barriers, of differing heights. This fit is better than a single exponential, but still does not follow the power law at long times.

The assumption of n distinct barriers is arbitrary; a more reasonable model would consider a continuous distribution of energy barriers for different single-molecule events, giving a survival probability distribution of the form (29),

$$P_{\text{survival}}(t) = \int_0^\infty g(E_b) e^{-\frac{t}{\tau}} dE_b, \tag{2}$$

where $g(E_b)$ is the probability density function of energy barrier heights and where E_b is related to τ by the Arrhenius relation: $\tau = \tau_D \exp[E_b/k_BT]$. The value τ_D is a diffusive timescale that is not determined in our experiments. Following Austin et al., the particular form of $g(E_b)$ may be found by fitting the survival probability data to an arbitrary function, and calculating its inverse Laplace transform (30). We fit our $P_{\text{survival}}(t)$ data using the Becquerel function, which has been previously used to describe kinetics of CO binding to myoglobin at low temperatures (30) and which has a known inverse Laplace transform. It fits our data well at short times and follows the observed power law region at long times,

$$P_{\text{survival}}(t) = (1 + t/\tau_0)^{-\alpha}, \tag{3}$$

where τ_0 and α are fit parameters. The inverse Laplace transform of Eq. 3 gives $g(E_b)$, the distribution function (30,31),

$$g(E_b) = \frac{\left[\tau_0 \Big/ \left(\tau_D \exp\left[\frac{E_b}{k_BT}\right]\right)\right]^\alpha \exp\left[-\tau_0 \Big/ \left(\tau_D \exp\left[\frac{E_b}{k_BT}\right]\right)\right]}{\Gamma(\alpha) k_BT}. \tag{4}$$

Without knowledge of τ_D, the absolute energy barrier height cannot be directly obtained from our data. We can, however, use the Arrhenius relation to express the energy barrier distribution in terms of τ, which we do know exactly, as

$$G(\tau) = \frac{(\tau_0/\tau)^\alpha \exp(\tau_0/\tau)}{\Gamma(\alpha) k_BT}. \tag{5}$$

Note that $G(\tau)$ is distinct from the timescale distribution; rather, it is the energy barrier distribution expressed in terms of τ (30). We are particularly interested in the peak of the distribution. We denote the timescale and energy barrier associated with the peak as τ^* and E_b^*, respectively, and use these as the starting point for subsequent analyses. Setting the derivative with respect to τ of Eq. 5 to zero and solving, we find that the timescale at the peak of the distribution is $\tau^* = \tau_0/\alpha$; we define E_b^* as the energy barrier associated with τ^*.

Using E_b^* as a point of reference, we can now plot Eq. 4 as $g(E_b\text{-}E_b^*)$. This shifts $g(E_b)$ on the E_b axis, but preserves its shape exactly. A plot of $g(E_b\text{-}E_b^*)$ for the 27-mer poly-dA molecule at 80 mV is shown in Fig. 2 *C*. Since the sole difference between $g(E_b)$ and $g(E_b\text{-}E_b^*)$ is a shift on the E_b axis, we will refer to $g(E_b)$ for the remainder of the discussion.

The energy barrier distribution contains information about the interactions that lead to nonexponential kinetics. Equation 4 is closely related to the Gamma distribution, which describes the distribution of waiting times for α events to occur in a Poisson process, generalized to noninteger values of α. This suggests that stochastic increases to the energy barrier height may result from infrequent binding events between the DNA and the pore, while noninteger values of α may reflect variations in binding energies for different interaction sites. The hypothesis of DNA-pore interactions is supported by experimentally measured DNA translocation rates through α-HL pores, which are more than an order-of-magnitude slower than velocities observed (32) in solid state nanopores or predicted in analytic and simulation studies (14). Further experimental work would be required to determine the exact mechanism at play, though it is known that hydrogen bond and salt bridge interactions between the phosphates of the DNA backbone and the amino group of lysine residues (present in the α-HL constriction) are common (33). We

therefore speculate that the energy barrier height distribution is caused by DNA-pore interactions, which differ from one escape event to the next.

The spread of the energy distribution is determined by the value of α (see Appendix B). Full width at half-maximum values (FWHM) for $g(E_b)$ ranged from $\sim 1\ k_BT$ ($\alpha \geq 5$) to $\sim 4.5\ k_BT$ ($\alpha = 0.35$) with values of $\sim 2.5\ k_BT$, equivalent to one hydrogen bond, being most common. Though the relationship was not perfect, energy spread tended to increase with the electrostatic energy barrier, suggesting that molecules held in the pore for longer times are subject to increased DNA-pore interactions (see Figs. 3 and 4). Energy spreads did not, however, correlate with molecule length.

We now turn our attention to the relationship between escape timescale and applied potential. For this analysis, we consider τ^*, the timescale associated with the maximum of the energy distribution, E_b^*. Addition of a potential-dependent term to the Arrhenius relation gives a Kramers' rule relationship between the applied potential and the escape timescale. Substituting the electrostatic potential energy barrier and dominant timescale into Kramers' law gives

$$\tau^* = \tau_D \exp\left[\frac{E_0}{k_BT} + V\frac{ze}{k_BT}\sum_{i=1}^{N}\frac{\Delta V_i}{V}\right]. \quad (6)$$

The first term in the exponential, E_0, is the energy barrier height in the absence of applied force, which depends on entropy effects and interactions between DNA and the pore. The second term is the electrostatic energy barrier: z is the effective charge per nucleotide, V is the applied electrostatic potential (positive when pulling the molecule into the pore), and $\Delta V_i/V$ is the fraction of the potential the i^{th} nucleotide must cross for the molecule to escape from the pore. Fig. 3 *A* shows data confirming the exponential relationship between escape timescale and applied potential for molecules ranging from 20- to 65-nt long.

The representation of the data in Fig. 3 *A* highlights the differences in escape kinetics arising from molecule length. Replotting the same timescale data versus electrostatic energy barrier height (E_V—see Appendix C for calculation) reveals a complex dependence on molecule length (see Fig. 3 *B*). E_V combines the effects of electrostatic force, charge of the molecule (proportional to length), and impact of pore geometry on the electric field. This is, in effect, normalization with respect to length that should collapse the data from different length molecules onto a single plot, assuming no other factors play a role in the escape timescale. Timescales for molecules $\leq$30-nt-long all exhibit similar dependence on E_V; however, timescales for longer molecules are also length-dependent. The reason for this length dependence is unclear, although it likely involves the portion of DNA that protrudes from the *trans*-side of the pore. Possible causes include DNA-lipid interactions, or the entropic cost of confining this portion of the DNA molecule as it moves through the pore.

The barrier height sensitivity to electrostatic potential (which we define as m) is the second term in Eq. 6 divided by V,

$$m = \sum_{i=1}^{N}\frac{ze\Delta V_i}{k_bTV}. \quad (7)$$

From the slope of the m versus N (Fig. 3 *A*, *inset*), we estimate the effective charge per nucleotide to be $0.4e$. Other estimates range from $\sim$0.1 (22,34) to $\sim$0.3 (11,35). None of these calculations separate effects of charge screening from effects of possible electroosmotic flow in the pore due to motion of the charge-carrying cations (34). Since electroosmotic flow would oppose the electrostatic force on DNA, z is likely to be underestimated in translocation experiments, but overestimated in our experiments (36). The intercept of m versus N is nonzero, which is reasonable, since not all nucleotides must pass across the entire electrostatic potential to escape from the pore.

CONCLUSION

We have shown that subtle energetic perturbations can have a profound effect on the kinetics of polynucleotide escape from nanopores. Nonexponential decay of the survival probability *vs.* time for molecules trapped in the pore indicates a typical spread in energy barrier height of $\sim 2.5\ k_BT$ for poly-dA, leading to long residence time in the pore for some molecules. A likely cause of this energy distribution is interaction between the bases of the DNA and the interior surface of the nanopore, though molecular dynamics or mutational studies will be required to determine precisely the source of the interactions.

Though conditions in our experiments were chosen to emphasize these effects, they also appear to be present in translocation experiments. Emerging nanopore technologies, such as single molecule sequencing, will require accurate stochastic models of DNA translocation to interpret results,

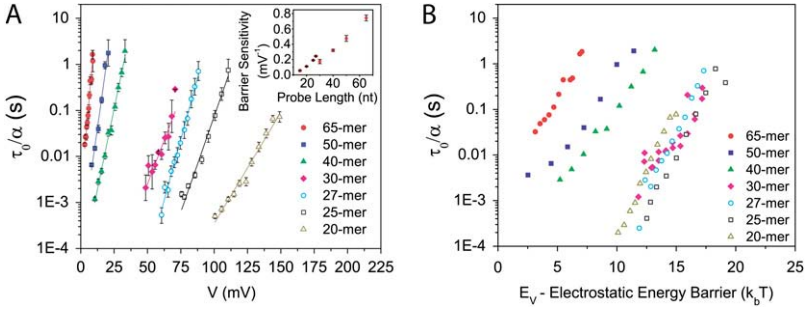

FIGURE 3 (*A*) Relationship between dominant escape timescale and barrier height for DNA strands of different lengths. Labels indicate polymer length in nucleotides. Lines are exponential fits to the data. Error bars indicate standard error of measurement, estimated using a bootstrap algorithm. (*Inset*) Barrier height sensitivity to electrostatic potential as a function of molecule length (see Eq. 7). Error bars indicate standard error of measurement, calculated by error propagation from data in the main figure. (*B*) Characteristic timescale for escape (τ_0/α) versus calculated electrostatic barrier, E_V (see Appendix C).

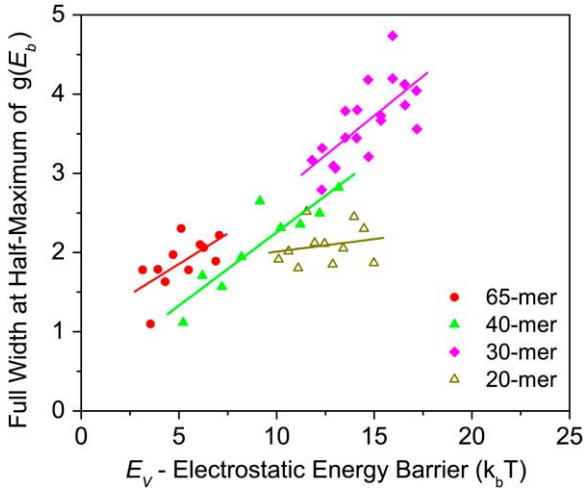

FIGURE 4 Full width at half-maximum (FWHM) of the energy barrier distribution $g(E_b)$ for DNA escape from the α-HL nanopore versus the calculated electrostatic energy barrier E_V. Lines are linear fits to the data (see Appendices B and C for calculations). The FWHM of $g(E_b)$ shows a trend of increasing with the electrostatic energy barrier (with the possible exception of the 20-mer dataset), but is not correlated to molecule length.

and should therefore consider the effect of anomalously long translocation times for some molecules. Design of synthetic nanopores, and in particular their surface chemistry, should also be guided by the understanding of stochastic binding effects in escape time or translocation time distributions.

APPENDIX A—FOKKER-PLANCK MODEL OF ESCAPE KINETICS

In our experiments, the DNA molecule escapes by diffusing along the axis of the pore, against an electrostatic force. We have developed a simple mathematical model of the escape process using the Fokker-Planck equation (Eq. 1). While this model is not sufficiently detailed to make quantitative predictions regarding kinetics, it is adequate for making qualitative predictions—specifically, that escape kinetics are expected to be exponential.

For DNA escape, we take $D = 2 \times 10^{-10}$ cm^2/s (16), and $\gamma = 1$ kg/s, which has been shown to be consistent with the high-friction regime (37). We model the energy barrier as a combination of electrostatic and entropic energies as

$$E(x) = \begin{cases} \dfrac{ze}{k_B T} xV & x \le L - N \\ \dfrac{ze}{k_B T}\left[x - \dfrac{(x - L + N)^2}{N}\right]V + \dfrac{x}{b} & x > L - N \end{cases}, \quad (8)$$

where $z = 0.4$ is the effective charge per nucleotide. All length terms are measured in nucleotides: L is the length of the DNA molecule, $N = 22$ nt is the length of the nanopore, x is the contour length of DNA that has escaped to the *cis*-side of the pore (equivalent to position), and $b = 2.5$ nt is the Kuhn length (38). The x/b term measures the increase in entropy as DNA escapes from the confinement of the pore, assumed to be 1 k_BT per Kuhn length (39). This expression ignores entropy changes from tethering the DNA strands on both the *cis*- and *trans*- sides of the pore; these have only a relatively minor effect on $E(x)$ ($\sim$1 k_BT). The energy barrier for a 27-mer DNA molecule at $V = 80$ mV is shown in Fig. 5.

We use an absorbing boundary at $x = L$, the point at which the probe has completely exited the pore and can diffuse away, and reflecting boundary at $x = 0$,

$$f(L,t) = 0;\ S(0,t) = 0.$$

$S(x,t)$ is the probability current such that

$$\frac{\partial S(x,t)}{\partial x} + \frac{\partial f(x,t)}{\partial t} = 0.$$

The initial condition is assumed to be

$$f(x,0) = \delta(x - x_{\min}).$$

Though thermal fluctuations and a small second derivative of $f(x,t)$ at $x = x_{\min}$ would violate this assumption, the nature of our experiment is such that the molecule is held tightly in the pore under a very strong electric field ($\sim$200 mV potential drop across the pore) before the sudden decrease in the barrier at $t = 0$. At this potential, a shift of 1 nucleotide corresponds to $\sim$2.5 k_BT increase in electrostatic potential energy, meaning that $>$99% of molecules will be within two nucleotides of $x = 0$ at the start of the experiment. This is a considerably tighter starting point distribution than previous similar escape experiments (18).

To obtain the survival probability of the probe in the pore, we integrate $f(x,t)$ on the interval ($0 < x < L$),

$$P_{\text{survival}}(t) = \int_0^L f(x,t)\,dx. \quad (9)$$

The Fokker-Planck equation does not generally have a closed-form analytic solution. We therefore determined the survival probability numerically, using a finite difference method.

Fig. 5 shows the survival probability for a 27-mer DNA molecule at an applied potential of 80 mV. At short times, the escape probability is nonexponential, since the system has not yet relaxed to a quasistationary state. At long times, however, escape kinetics are exponential. We note that the model predicts exponential kinetics at long times regardless of the barrier height, or relative contributions from entropy and electrostatic potential. This suggests that the Fokker-Planck model neglects some critical aspect of the system—namely fluctuations in the energy barrier height caused by DNA-pore interactions.

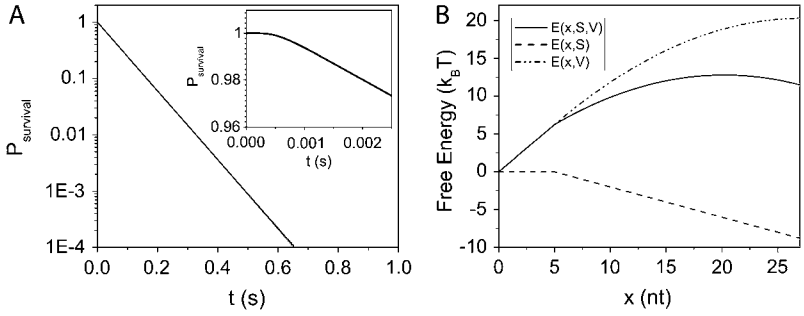

FIGURE 5 Fokker-Planck model of DNA escape. All data shown is calculated for a 27-mer DNA molecule trapped in the pore by an 80-mV applied potential. (*A*) Survival probability as a function of time, calculated by numerical integration of the Fokker-Planck equation. (*Inset*) At short times, survival probability is nonexponential (same data as main figure). (*B*) Potential energy as calculated from Eq. 8. Note that $E(x,V)$ is the applied potential contribution to free energy; $E(x,S)$ is the entropic contribution to free energy, and $E(x,V,S) = E(x,V) + E(x,S)$.

APPENDIX B: CALCULATION OF ENERGY SPREAD FROM ESCAPE TIMESCALE DISTRIBUTIONS

The position and width of the energy barrier distribution probably increase by separate mechanisms as the potential increases, since they are estimated by different combinations of fitting parameters. The width of $g(E_b)$ is independent from τ_0, and can be estimated using α alone. We demonstrate this using the separation of the inflection points, which occur at

$$E_b = \ln\left(\frac{1}{2}\frac{(2\alpha + 1 \pm \sqrt{4\alpha + 1})\tau_0}{\alpha^2 \tau_D}\right). \quad (10)$$

The separation of the inflection points is, therefore,

$$\Delta E_b = k_b T \ln\left(\frac{2\alpha + 1 + \sqrt{4\alpha + 1}}{2\alpha + 1 - \sqrt{4\alpha + 1}}\right). \quad (11)$$

This demonstrates that variation in the energy distribution's width is not simply an artifact of changing the dominant energy barrier. We speculate that molecules experiencing a larger energy barrier have longer (average) residence times, and thus, more opportunities to bind to the pore. This, in turn, causes a greater increase in the width of the energy barrier.

APPENDIX C—CALCULATION OF ELECTROSTATIC POTENTIAL ENERGY FOR DNA IN THE NANOPORE

We estimate E_V as

$$E_V = \frac{ze}{k_b T}\sum_{i=1}^{N} \Delta V_i, \quad (12)$$

where N is the number of nucleotides in the polymer. ΔV_i is the potential difference the i^{th} nucleotide must pass through to escape from the pore, and is calculated on the following assumptions: the vestibule and β-barrel of the α-HL pore each contain 15 nucleotides (40). Based on a molecular dynamics simulation of DNA in the pore, we assume that 20% of the potential drop occurs in the vestibule, with the remaining 80% of the potential drop in the β-barrel (41). For short molecules that do not extend all the way through the pore, we assume that the potential drop occurs entirely across the region of the pore occupied by the DNA strand, since impedance has been shown to be relatively insensitive to length for molecules extending only partway through the pore (42). Note that $z = 0.4$ is the effective charge per nucleotide (see Results and Discussion, and (11)). For calculations in Fig. 3 *B*, we have made the simplifying assumption that z is identical for nucleotides inside (z_{in}) and outside (z_{out}) the pore. Though this is not necessarily true, escape timescales of short molecules are dependent only on E_V, while escape timescales of long molecules are dependent on both length and E_V, regardless of the values chosen for z_{in} and z_{out}.

Thanks to Dhruti Trivedi, David Broemeling, Jason R. Dwyer, Dylan Gunn, and Benjamin Smith for helpful discussions.

This work was supported by National Human Genome Research Institute grant No. R01HG003248. Thanks to the Natural Sciences and Engineering Research Council of Canada for student funding (M.J.W.) and Le Fonds Québécois de la Recherche sur la Nature et les Technologies for postdoctoral funding (V.T.-C.).

REFERENCES

1. Healy, K. 2007. Nanopore-based single-molecule DNA analysis. *Nanomedicine*. 2:459–481.
2. Meller, A. 2003. Dynamics of polynucleotide transport through nanometer-scale pores. *J. Phys. Condens. Mat.* 15:R581–R607.
3. Nakane, J. J., M. Akeson, and A. Marziali. 2003. Nanopore sensors for nucleic acid analysis. *J. Phys. Condens. Mat.* 15:R1365–R1393.
4. Kasianowicz, J. J., E. Brandin, D. Branton, and D. W. Deamer. 1996. Characterization of individual polynucleotide molecules using a membrane channel. *Proc. Natl. Acad. Sci. USA*. 93:13770–13773.
5. Deamer, D. W., and M. Akeson. 2000. Nanopores and nucleic acids: prospects for ultrarapid sequencing. *Trends Biotechnol.* 18:147–151.
6. Deamer, D. W., and D. Branton. 2002. Characterization of nucleic acids by nanopore analysis. *Acc. Chem. Res.* 35:817–825.
7. Akeson, M., D. Branton, J. J. Kasianowicz, E. Brandin, and D. W. Deamer. 1999. Microsecond timescale discrimination among polycytidylic acid, polyadenylic acid, and polyuridylic acid as homopolymers or as segments within single RNA molecules. *Biophys. J.* 77:3227–3233.
8. Meller, A., L. Nivon, E. Brandin, J. Golovchenko, and D. Branton. 2000. Rapid nanopore discrimination between single polynucleotide molecules. *Proc. Natl. Acad. Sci. USA*. 97:1079–1084.
9. Gracheva, M. E., A. L. Xiong, A. Aksimentiev, K. Schulten, G. Timp, and J. P. Leburton. 2006. Simulation of the electric response of DNA translocation through a semiconductor nanopore-capacitor. *Nanotechnology*. 17:622–633.
10. Lagerqvist, J., M. Zwolak, and M. Di Ventra. 2006. Fast DNA sequencing via transverse electronic transport. *Nano Lett.* 6:779–782.
11. Nakane, J., M. Wiggin, and A. Marziali. 2004. A nanosensor for transmembrane capture and identification of single nucleic acid molecules. *Biophys. J.* 87:615–621.
12. Tropini, C., and A. Marziali. 2007. Multi-nanopore force spectroscopy for DNA analysis. *Biophys. J.* 92:1632–1637.
13. Zhao, Q., G. Sigalov, V. Dimitrov, B. Dorvel, U. Mirsaidov, S. Sligar, A. Aksimentiev, and G. Timp. 2007. Detecting SNPs using a synthetic nanopore. *Nano Lett.* 7:1680–1685.
14. Lubensky, D. K., and D. R. Nelson. 1999. Driven polymer translocation through a narrow pore. *Biophys. J.* 77:1824–1838.
15. Fologea, D., J. Uplinger, B. Thomas, D. S. McNabb, and J. L. Li. 2005. Slowing DNA translocation in a solid-state nanopore. *Nano Lett.* 5:1734–1737.
16. Mathe, J., A. Aksimentiev, D. R. Nelson, K. Schulten, and A. Meller. 2005. Orientation discrimination of single-stranded DNA inside the α-hemolysin membrane channel. *Proc. Natl. Acad. Sci. USA*. 102:12377–12382.
17. Meller, A., and D. Branton. 2002. Single molecule measurements of DNA transport through a nanopore. *Electrophoresis*. 23:2583–2591.
18. Bates, M., M. Burns, and A. Meller. 2003. Dynamics of DNA molecules in a membrane channel probed by active control techniques. *Biophys. J.* 84:2366–2372.
19. Muthukumar, M., and C. Y. Kong. 2006. Simulation of polymer translocation through protein channels. *Proc. Natl. Acad. Sci. USA*. 103:5273–5278.
20. Kantor, Y., and M. Kardar. 2004. Anomalous dynamics of forced translocation. *Phys. Rev. E Stat. Nonlin. Soft Matter Phys.* 69:021806.
21. Matysiak, S., A. Montesi, M. Pasquali, A. B. Kolomeisky, and C. Clementi. 2006. Dynamics of polymer translocation through nanopores: theory meets experiment. *Phys. Rev. Lett.* 96:118103.
22. Sauer-Budge, A. F., J. A. Nyamwanda, D. K. Lubensky, and D. Branton. 2003. Unzipping kinetics of double-stranded DNA in a nanopore. *Phys. Rev. Lett.* 90:238101.
23. Mathe, J., H. Visram, V. Viasnoff, Y. Rabin, and A. Meller. 2004. Nanopore unzipping of individual DNA hairpin molecules. *Biophys. J.* 87:3205–3212.
24. Hanggi, P., P. Talkner, and M. Borkovec. 1990. Reaction-rate theory—50 years after Kramers. *Rev. Mod. Phys.* 62:251–341.
25. Vercoutere, W. A., S. Winters-Hilt, V. S. DeGuzman, D. Deamer, S. E. Ridino, J. T. Rodgers, H. E. Olsen, A. Marziali, and M. Akeson. 2003. Discrimination among individual Watson-Crick base pairs at the termini of single DNA hairpin molecules. *Nucleic Acids Res.* 31:1311–1318.
26. Butler, T. Z., J. H. Gundlach, and M. Troll. 2007. Ionic current blockades from DNA and RNA molecules in the α-hemolysin nanopore. *Biophys. J.* 93:3229–3240.

27. Wanunu, M., B. Chakrabarti, J. Mathe, D. R. Nelson, and A. Meller. 2008. Orientation-dependent interactions of DNA with an α-hemolysin channel. *Phys. Rev. E Stat. Nonlin. Soft Matter Phys.* 77:031904.

28. Risken, H. 1984. The Fokker-Planck Equation. Springer-Verlag, New York.

29. Xie, X. S. 2002. Single-molecule approach to dispersed kinetics and dynamic disorder: probing conformational fluctuation and enzymatic kinetics. *J. Chem. Phys.* 117:11024–11032.

30. Austin, R. H., K. W. Beeson, L. Eisenstein, H. Frauenfelder, and I. C. Gunsalus. 1975. Dynamics of ligand-binding to myoglobin. *Biochemistry.* 14:5355–5373.

31. Berberan-Santos, M. N., E. N. Bodunov, and B. Valeur. 2005. Mathematical functions for the analysis of luminescence decays with underlying distributions: 2. Becquerel (compressed hyperbola) and related decay functions. *Chem. Phys.* 317:57–62.

32. Chen, P., J. J. Gu, E. Brandin, Y. R. Kim, Q. Wang, and D. Branton. 2004. Probing single DNA molecule transport using fabricated nanopores. *Nano Lett.* 4:2293–2298.

33. Nadassy, K., S. J. Wodak, and J. Janin. 1999. Structural features of protein-nucleic acid recognition sites. *Biochemistry.* 38:1999–2017.

34. Zhang, J. S., and B. I. Shklovskii. 2007. Effective charge and free energy of DNA inside an ion channel. *Phys. Rev. E Stat. Nonlin. Soft Matter Phys.* 75:021906.

35. Keyser, U. F., J. van der Does, C. Dekker, and N. H. Dekker. 2006. Optical tweezers for force measurements on DNA in nanopores. *Rev. Sci. Instrum.* 77:105105.

36. Luan, B., and A. Aksimentiev. 2008. Electro-osmotic screening of the DNA charge in a nanopore. *Phys. Rev. E Stat. Nonlin. Soft Matter Phys.* 78. Accepted.

37. Huopaniemi, I., K. Luo, and T. Ala-Nissila. 2006. Langevin dynamics simulations of polymer translocation through nanopores. *J. Chem. Phys.* 125:124901.

38. Smith, S. B., Y. J. Cui, and C. Bustamante. 1996. Overstretching B-DNA: the elastic response of individual double-stranded and single-stranded DNA molecules. *Science.* 271:795–799.

39. Flomenbom, O., and J. Klafter. 2003. Single stranded DNA translocation through a nanopore: a master equation approach. *Phys. Rev. E Stat. Nonlin. Soft Matter Phys.* 68:041910.

40. Song, L. Z., M. R. Hobaugh, C. Shustak, S. Cheley, H. Bayley, and J. E. Gouaux. 1996. Structure of staphylococcal α-hemolysin, a heptameric transmembrane pore. *Science.* 274:1859–1866.

41. Wells, D. B., V. Abramkina, and A. Aksimentiev. 2007. Exploring transmembrane transport through α-hemolysin with grid-steered molecular dynamics. *J. Chem. Phys.* 127:125101.

42. Howorka, S., and H. Bayley. 2002. Probing distance and electrical potential within a protein pore with tethered DNA. *Biophys. J.* 83:3202–3210.